10. Portigal, D. L. & Burstein, E. Magneto-spatial dispersion effects on the propagation of electromagnetic radiation in crystals. *J. Phys. Chem. Solids* **32**, 603–608 (1971).
11. Baranova, N. B., Bogdanov, Yu. V. & Zeldovich, B. Ya. Electrical analog of the Faraday effect and other new optical effects in liquids. *Opt. Commun.* **22**, 243–247 (1977).
12. Baranova, N. B. & Zeldovich, B. Ya. Theory of a new linear magnetorefractive effect in liquids. *Mol. Phys.* **38**, 1085–1098 (1979).
13. Rau, H. Asymmetric photochemistry in solution. *Chem. Rev.* **83**, 535–547 (1983).
14. Inoue, Y. Asymmetric photochemical reactions in solution. *Chem. Rev.* **92**, 741–770 (1992).
15. Barron, L. D. & Vrbancich, J. Magneto-chiral birefringence and dichroism. *Mol. Phys.* **51**, 715–730 (1984).
16. Stevenson, K. L. & Verdieck, J. F. Partial photoresolution II. Application to some chromium complexes. *Mol. Photochem.* **1**, 271–288 (1969).
17. McCaffery, A. J., Mason, S. F. & Ballard, R. E. Optical rotatory power of coordination compounds. Part III The absolute configurations of trigonal metal complexes. *J. Chem. Soc.* 2883–2892 (1965).
18. McCaffery, A. J., Stephens, P. J. & Schatz, P. N. The magnetic optical activity of d — d transitions. Octahedral chromium(III), cobalt(III), nickel(II) and manganese(II) complexes. *Inorg. Chem.* **6**, 1614–1625 (1967).
19. Pracejus, H. Asymmetrische Synthesen. *Fortschr. Chem. Forsch.* **8**, 493–553 (1967).
20. Bernstein, W. J. The attempted asymmetric synthesis of helicenes by photolysis under magnetic field. Thesis, Lawrence Berkeley Labs (1972).
21. Teutsch, H. Zur Enstehung optischer Aktivität in der Biosphäre: Ausgewählte Photoreaktionen als asymmetrischen Synthesen. Thesis, Univ. Bremen (1988).
22. Wagniere, G. & Meier, A. Difference in the absorption coefficient of enantiomers for arbitrarily polarized light in a magnetic field—A possible source of chirality in molecular evolution. *Experientia* **39**, 1090–1091 (1983).
23. Engel, M. H. & Macko, S. A. Isotopic evidence for extraterrestial non-racemic amino acids in the Murchison meteorite. *Nature* **389**, 265–268 (1997).
24. Bailey, J. *et al.* Circular polarization in star-formation regions: Implications for biomolecular homochirality. *Science* **281**, 672–674 (1998).
25. Lyne, A. G. Origins of the magnetic fields of neutron stars. *Nature* **308**, 605–606 (1984).

Acknowledgements

We thank H. Krath for technical assistance; P. Wyder, G. Martinez and B. van Tiggelen for comments on the manuscript; W. A. Bonner for providing important information; L. Barron for discussions; and B. Malezieux for synthesizing the pure enantiomers. The Grenoble High Magnetic Field Laboratory is a "laboratoire conventionné aux universités UJF et INP de Grenoble".

Correspondence and requests for materials should be addressed to G.L.J.A.R. (e-mail: rikken@polycnrs-gre.fr).

Reduced North Atlantic Deep Water flux to the glacial Southern Ocean inferred from neodymium isotope ratios

Randye L. Rutberg*†, Sidney R. Hemming* & Steven L. Goldstein*

** Lamont-Doherty Earth Observatory and Department of Earth and Environmental Sciences, Columbia University, Palisades, New York 10964, USA*

The global circulation of the oceans and the atmosphere transports heat around the Earth. Broecker and Denton[1] suggested that changes in the global ocean circulation might have triggered or enhanced the glacial–interglacial cycles. But proxy data for past circulation taken from sediment cores in the South Atlantic Ocean have yielded conflicting interpretations of ocean circulation in glacial times—$\delta^{13}C$ variations in benthic foraminifera[2–6] support the idea of a glacial weakening or shutdown of North Atlantic Deep Water production, whereas other proxies, such as Cd/Ca, Ba/Ca and $^{231}Pa/^{230}Th$ ratios, show little change from the Last Glacial Maximum to the Holocene epoch[7–9]. Here we report neodymium isotope ratios from the dispersed Fe–Mn oxide component of two southeast Atlantic sediment cores. Both cores show variations that tend towards North Atlantic signatures during the warm marine isotope stages 1 and 3, whereas for the full glacial stages 2 and 4 they are closer to Pacific Ocean signatures. We conclude that the export of North Atlantic Deep Water to the Southern Ocean has resembled present-day conditions during the warm climate intervals, but was reduced during the cold stages. An increase in biological productivity may explain the various proxy data during the times of reduced North Atlantic Deep Water export.

In the present 'conveyor' mode, deep water formed in the North Atlantic flows southwards to the circum-Antarctic Southern Ocean. Circumpolar waters flow to the Indian and Pacific oceans, where they upwell and return to the North Atlantic as intermediate and surface waters. The warm and salty northward-flowing surface water releases heat, maintaining mild temperatures in Europe. Whether the conveyor operated during full glacial stages is still an open question, due to the conflicting signals from palaeocirculation proxies in South Atlantic sediments. The importance of ocean circulation in modulating the global climate warrants the use of additional proxies to resolve this conflict.

Neodymium isotope ratios (ϵ_{Nd}; see Table 1) in sea water and marine precipitates have characteristics that make them powerful palaeoceanographic tracers. They are distinct in different ocean basins, with the highest values in the Pacific ($\epsilon_{Nd} = 0$ to -4) and the lowest values in the North Atlantic ($\epsilon_{Nd} \approx -14$), broadly reflecting the ages of the surrounding continents (see refs 10, 11 and references therein). Circum-Antarctic Nd isotope ratios are intermediate, consistent with mixing of Atlantic- and Pacific-derived waters[11–13]. Like stable-isotope and trace-element proxies, Nd isotope variations in sea water can be directly related to water masses in depth profiles (see, for example, refs 12–16). However, Nd isotope ratios are not measurably fractionated by biological processes or temperature. Therefore, in situations where these effects may cause complications with conventional tracers, the Nd isotope signatures of the source waters are conserved. In the outer layers of Fe–Mn crusts and nodules, Nd isotopes show systematic geographical variations consistent with present-day deep-water circulation[10]. However,

Table 1 South Atlantic cores Nd isotope data

Depth in core (cm)	Age (kyr)	$^{143}Nd/^{144}Nd$	ϵ_{Nd}
RC11-83			
25	2.5	0.512208 ± 09	−8.39 ± 0.18
126	8.9	0.512180 ± 07	−8.93 ± 0.14
249	14.3	0.512261 ± 12	−7.35 ± 0.23
398	19.7	0.512310 ± 11	−6.40 ± 0.21
600	25.4	0.512296 ± 07	−6.67 ± 0.14
780	33.1	0.512236 ± 21	−7.84 ± 0.41
839	35.8	0.512234 ± 09	−7.88 ± 0.18
999	44.0	0.512185 ± 10	−8.84 ± 0.20
1,101	49.9	0.512204 ± 13	−8.49 ± 0.20
1,251	59.7	0.512260 ± 10	−7.37 ± 0.20
1,285	62.1	0.512271 ± 14	−7.16 ± 0.27
1,381	67.4	0.512224 ± 07	−8.08 ± 0.14
TNO57-6PC			
15	Holocene	0.512222 ± 18	−8.11 ± 0.35
60	Stage 2	0.512432 ± 11	−4.02 ± 0.21

RC11-83 is a dry core from the LDEO Core Repository; TNO57-6PC is a wet core from the ODP Repository at LDEO. Fe–Mn oxide fractions of sediments were leached using hydroxylamine hydrochloride following dissolution of the carbonate fraction with buffered acetic acid. Rare-earth elements (REE) were isolated using TruSpec resin, and Nd was separated using α-hydroxyisobutyric acid and cation resin. The procedural Nd blank is ~250 pg, which ranges from 0.2% to 0.8% of the total Nd in each sample, and is thus negligible. Nd was measured by dynamic multicollection as NdO⁺ on a VG (Micromass) Sector 54 mass spectrometer at LDEO. $^{143}Nd/^{144}Nd$ ratios were normalized to $^{146}Nd/^{144}Nd = 0.7219$ and adjusted to a value of 0.511860 for the La Jolla Nd standard. Reported errors are in-run $2\sigma_{mean}$. The average La Jolla measured values over two measurement periods were 0.511835 ± 22 (2σ external reproducibility, $n = 12$), and 0.511848 ± 23 ($n = 19$), and these (±0.44 ϵ_{Nd} units) are taken as the errors. Sample RC11-83 at 1,101 cm was measured as Nd⁺ by static multicollection on a Micromass P-54 Sector Multicollector ICP-MS at LDEO. The average measured La Jolla value was 0.511862 ± 8 (2σ external reproducibility, $n = 8$). ϵ_{Nd} is the deviation of measured $^{143}Nd/^{144}Nd$ ratios from the bulk Earth value of $^{143}Nd/^{144}Nd = 0.512638$ in parts per 10^4. Errors in the $^{143}Nd/^{144}Nd$ ratios are in the fifth place after the decimal point.

† Present address: Department of Geography, Hunter College of CUNY, 695 Park Avenue, New York, New York 10021, USA.

their slow accumulation rates of a few mm per Myr limit their usefulness to the tracking of ocean circulation changes over glacial–interglacial timescales.

Fe–Mn oxides precipitate from the water column as coatings on biogenic and detrital phases and as particles. To the extent that their Nd isotope ratios record and retain deep-water compositions, they can be directly integrated with high-resolution proxy records in sediment cores. Thus, unlike Fe–Mn nodules and crusts, deep-sea cores allow study of ocean circulation over sub-glacial timescales.

We report downcore Nd isotope data from the dispersed Fe–Mn oxide component of two southeast Atlantic cores. RC11-83 (40° 36′ S, 9° 48′ E, 4,718 m, ~25 cm kyr^{-1}) is from the Cape basin. TNO57-6PC (42° 55′ S, 8° 53′ E, 3,750 m, ~15 cm kyr^{-1}) is from south of the Cape basin. Both lie slightly north of the Subpolar Front. RC11-83, extending from the Holocene to the marine isotope stage (MIS) 4–5 transition at ~70 kyr, is one of the most intensively studied cores in the South Atlantic, with a detailed ^{14}C chronology and stable-isotope record[4,6]. Variations in benthic foraminiferal δ^{13}C (Fig. 1) have been interpreted to indicate a reduced flux of North Atlantic Deep Water (NADW) to the South Atlantic during the last glacial maximum (LGM) and MIS 4.

The Fe–Mn component of samples was isolated using a leaching procedure (Table 1). High-sedimentation-rate cores were sampled in order to minimize possible pore water smearing effects of the Fe–Mn signal over significant time intervals represented in the cores. The integrity of the marine signal was tested in two ways. Firstly, all of the leachates have Quaternary seawater values of $^{87}Sr/^{86}Sr$ = 0.70919–0.70922. Coexisting silicate detritus values of 0.717–0.723 (S.L.G., S.R.H., S. Kish and R.L.R., unpublished data) are so much higher than sea water that a tiny amount of detrital contamination of the Fe–Mn leachates would be easily detected. The marine Sr isotope values provide strong evidence that we recovered the seawater signal for Sr. While this does not guarantee a seawater Nd signal, Nd is less soluble than Sr and less likely to experience cross-contamination from detritus. A second test is based on relationships between deep Atlantic seawater Nd isotopes and dissolved silica (Fig. 2a), using silica as an index of mixing between NADW (low SiO_2) and water derived from the Southern Ocean (high SiO_2). They show an excellent correlation, strongly indicating that Nd isotope variations in the deep Atlantic primarily reflect mixing of northern- and southern-derived waters. Nd isotope ratios of Holocene Fe–Mn leachates from the two cores, plotted against the SiO_2 content of the overlying bottom water[17], lie on this correlation. We conclude from these tests that the Nd isotopes in the Fe–Mn leachates faithfully record the bottom water.

Downcore in RC11-83, Nd isotopes of the Fe–Mn leachates follow the benthic foraminiferal δ^{13}C variations (Fig. 1). They vary cyclically with climate stages, with the lowest values in the Holocene and MIS 3 ($\epsilon_{Nd} \approx -9$), higher values during the LGM and MIS 4 (reaching $\epsilon_{Nd} \approx -6$), and intermediate values during MIS transitions. Two analyses from the southerly core TNO57-6 show the same Holocene–LGM pattern but a larger difference. Its Holocene ϵ_{Nd} value is similar to that of RC11-83. The deep water at these sites is mainly Circumpolar Deep Water (CDW) from the Antarctic Circumpolar Current (ACC), but the dissolved SiO_2 is lower than Drake Passage CDW (Fig. 2a), indicating the presence of an additional component derived from the North Atlantic. This is fully consistent with the lower ϵ_{Nd} values of the Holocene Fe–Mn leachates compared to Drake Passage CDW (ref. 12). Although TNO57-6 is located only ~2° to the south of RC11-83, its LGM value of $\epsilon_{Nd} = -4.02$ is significantly higher than that of RC11-83. Both cores lie slightly north of the southeast Atlantic–Circumpolar transition zone, reflected by sharp vertical and latitudinal gradients in dissolved SiO_2 (ref. 17). We speculate that the larger offset of the LGM ϵ_{Nd} values between the cores, in contrast to the similarity in Holocene values, may reflect a northward shift of the transition

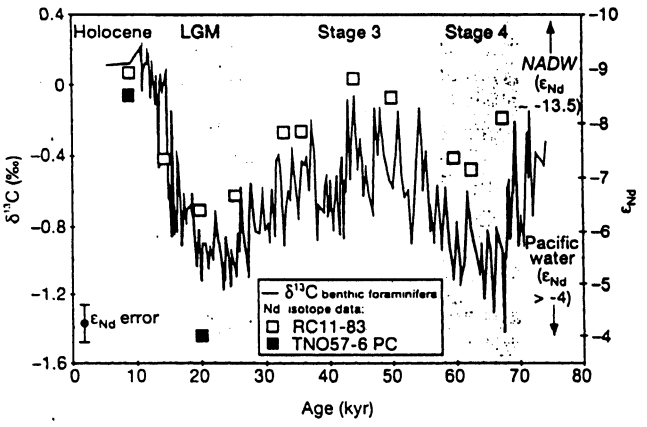

Figure 1 $^{143}Nd/^{144}Nd$ ratios of Fe–Mn leachates and benthic foraminiferal δ^{13}C versus age. Ages and δ^{13}C values for RC11-83 (left axis) are from refs 4 and 6. Holocene and LGM samples for TNO57-6PC are based on the stable-isotope stratigraphy (D. Hodell, personal communication) and not meant to correspond to the precise age. The Nd isotope data (right axis) corroborate the δ^{13}C evidence for glacial–interglacial changes in the NADW component at these sites. Core TNO57-6 shows a more extreme excursion towards Pacific-like ϵ_{Nd} values during the LGM.

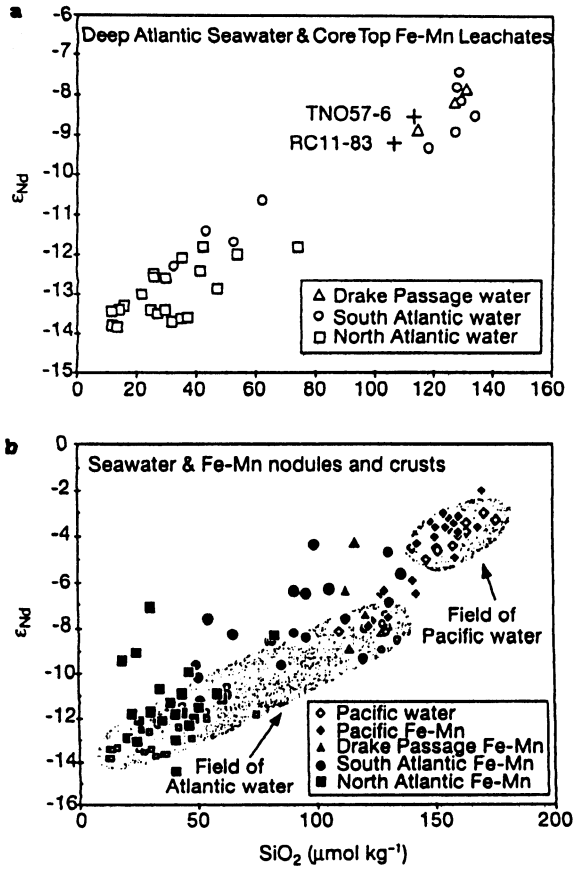

Figure 2 Dissolved silica versus Nd isotope ratios. **a**, ϵ_{Nd} values of dissolved Nd in deep seawater and in South Atlantic core-top Fe–Mn leachates. The leachate data are plotted against bottom-water dissolved silica at the site[17], and fall on the Atlantic seawater trend. **b**, ϵ_{Nd} in deep seawater and in Fe–Mn nodules and crusts. The Fe–Mn samples are plotted against bottom-water dissolved silica at the same sites[17]. Each Fe–Mn nodule and crust sample averages over several glacial–interglacial cycles. Most North Atlantic and Pacific Fe–Mn samples fall on the modern seawater trend. South Atlantic samples fall off the trend. Seawater and Fe–Mn data are from the literature.

zone, with southerly core TNO57-6 fully within CDW but RC11-83 still within the transition. The gradient's LGM location may be partly affected by the Agulhas ridge, with ~2,000 m of relief, which restricts deep-water flow into the Cape basin[18].

Atlantic trace-element and stable-isotope records have been interpreted to indicate a glacial shallowing of NADW[7,19], or a decrease in the NADW formation rate[2-6] during cold climate stages. The LGM values in both cores are higher than present-day Circumpolar seawater values (ϵ_{Nd} = −7 to −9). In the southerly core TNO57-6, the LGM value of ϵ_{Nd} = −4.02 indicates that deep Circumpolar waters had Pacific-like Nd isotope ratios.

The vigour of modern-day ACC flow and the efficiency of vertical mixing are reflected by nearly constant Nd isotope ratios in depth profiles from the Drake Passage[12]. Higher Nd isotope ratios in glacial Circumpolar water indicate a larger Pacific Nd component. However, it has been suggested that NADW may have survived as a coherent intermediate-depth water mass in the ACC during full glacial stages[20]. If the ACC was stratified, then glacial Circumpolar Deep Water might show a reduced NADW signal due to inefficient vertical mixing, rather due to than a change in the NADW flux to the Southern Ocean. In the modern-day ACC, the low-SiO_2 'tongue' of NADW can be traced in water column profiles of the Atlantic sector of the Southern Ocean only as far as ~55° E in the western Indian sector[17]. Thus, in order for NADW to survive as a coherent water mass around the entire Circumpolar perimeter, an ACC flow regime drastically different from today would be required. A glacial ACC more sluggish than the modern-day is directly at odds with conclusions of a recent study[21]. It is more likely that the reduced influence of Nd derived from the North Atlantic during full glacial stages is a consequence of decreased export of NADW.

Although our data support reduced NADW export to the Southern Ocean during cold climate stages, we have considered alternative possibilities. These include an additional source of Nd to the South Atlantic, a shorter glacial residence time of deep Atlantic Nd (resulting in a smaller NADW-Nd flux reaching the ACC despite a robust NADW-water flux), or changes in the Nd isotope ratio of the NADW or Pacific end-members. We now consider these three alternatives.

Antarctic ice cores show an increased aeolian dust flux derived from Patagonia during MIS 2 and 4[22]. If the higher particle flux scavenged dissolved Nd from NADW more efficiently during the LGM than today, the strength of the NADW ϵ_{Nd} signal could have been diminished even if the water flux remained constant. The Pacific-like LGM ϵ_{Nd} of sourtherly core TNO57-6 requires that enhanced scavenging in the Atlantic effectively extracted all of the Nd before the NADW reached the ACC. However, higher glacial dust input to the Pacific would have had the same enhanced scavenging effect on dissolved Nd. If deep water Nd concentrations decreased in both end-members, the Nd isotope ratios of mixtures would be conserved. Alternatively, if the Patagonian dust equilibrated with deep seawater, its high ϵ_{Nd} (= −3 to +8; ref. 23) could serve as a source of radiogenic Nd in the South Atlantic and ACC. However, in the modern north Pacific, where the aeolian component from China loess ($\epsilon_{Nd} \approx -10$) dominates the terrigenous input[24], Fe–Mn crusts and nodules reflect local bottom water having much higher values ($\epsilon_{Nd} \approx -4 \pm 2$). In the North Atlantic there is negligible exchange between deep waters and sinking particles 'armoured' by organic material[25]. Enhanced dust flux has been linked to productivity increases, which would increase the biological packaging of particles, and further inhibit isotopic exchange with sea water[26]. Thus it is unlikely that enhanced dust fluxes caused the glacial increase of South Atlantic deep-water ϵ_{Nd} values.

Local input from Antarctica could also influence Circumpolar Nd isotope ratios. There are no published Nd isotope analyses of water or sediments near Antarctica, hence Antarctic control on Southern Ocean water cannot be definitively precluded. However, the strong dissolved SiO_2–ϵ_{Nd} correlation in the modern Atlantic (Fig. 2a) shows that deep-water masses retain characteristic Nd isotope signatures over long travel paths. Nd isotopes in the ACC, intermediate to the North Atlantic and Pacific, are consistent with mixing of these sources, arguing against input from Antarctica as the controlling factor in the Southern Ocean.

Changes in ϵ_{Nd} of the Pacific or Atlantic end-members would also result in changes in the ACC. In the equatorial Pacific, a Fe–Mn crust in which glacial–interglacial timescales are resolvable shows constant ϵ_{Nd} of about −4 through stages 1–6[27]. Nd isotope ratios in the sampled outer layers of most other Fe–Mn nodules represent averages over 10^5–10^6 years, encompassing several glacial cycles. Pacific and most North Atlantic data, plotted against SiO_2 of bottom waters, lie on the modern seawater dissolved SiO_2–ϵ_{Nd} trend (Fig. 2b). In contrast, most South Atlantic data are offset to high ϵ_{Nd} values and thus more Pacific-like than expected from the modern-day bottom-water silica abundance. Thus the available Fe–Mn data indicate that the North Atlantic and Pacific end-members remained stable through the late Pleistocene, and that the South Atlantic, on average, had a larger Pacific component than today.

How sensitive are ACC Nd isotope ratios to NADW flux changes? Mass balance of Nd in the Southern Ocean—assuming an ACC volume of 1.5×10^{17} kg, a Holocene NADW flux of 22 Sv with ϵ_{Nd} = −13.5 and Nd = 22 pmol l^{-1}, and a Pacific flux of 18 Sv with ϵ_{Nd} = −4.5 and Nd = 42 pmol l^{-1} (refs 15, 16, 28, 29)—gives a reasonable ACC water residence time (120 yr) and Nd isotope ratio (ϵ_{Nd} = −8.4)[12,13]. Because of the short residence time of Circumpolar water, ACC Nd isotope ratios respond to input changes within hundreds of years. If the NADW flux decreased by 50% during the LGM, then the ϵ_{Nd} of the ACC increases only to −7.0, insufficient to account for the LGM values (Fig. 1). The present-day NADW value (ϵ_{Nd} = −13.5) is a mixture of sources from the Labrador Sea ($\epsilon_{Nd} \approx -20$) and the Denmark Straits and the Norwegian Sea ($\epsilon_{Nd} \approx -9$)[14,15]. If the glacial NADW flux was same as today, but the ϵ_{Nd} of NADW increased to −9 (that is, no Labrador Sea component), then the ACC ϵ_{Nd} value increases to −6.4, again much lower than the LGM value of southerly core TNO57-6. Although the real system is more complicated, some situations are implicit in these scenarios. For example, enhanced loss of NADW Nd in the LGM due to a higher scavenging efficiency follows the same mass balance scenario as a decreased NADW flux. A robust outcome of the mass balance is that an ϵ_{Nd} value of ≈ −5 for the glacial ACC cannot be attained by moderate perturbations to the system. Rather, unless the ϵ_{Nd} of the NADW and Pacific end-members both increased (unsupported by data), or there was an additional high-ϵ_{Nd} source of Nd to the South Atlantic or ACC (unconstrained by data), then the high LGM Nd isotope ratios indicate a drastic decrease in the glacial export of NADW.

The Nd isotope data support interpretations that LGM $\delta^{13}C$ values of benthic foraminifera in RC11-83 and other South Atlantic cores[2-6] reflect a much-reduced NADW flux to the South Atlantic. However, these conclusions conflict with the no-change interpretations based on Cd/Ca, Ba/Ca and $^{231}Pa/^{230}Th$ ratios[8,9,30]. If the NADW flux decreased, then alternative explanations are required to explain these data. Charles *et al.*[6] note that the $\delta^{13}C$ decrease in RC11-83 during the LGM of 1.2‰ (Fig. 1) is more than double that expected from a complete shutdown of NADW. They propose a combined change in thermohaline circulation and an increase in export productivity. Oxidation of the increased amount of organic matter would provide a pool of isotopically light carbon, in which case the low $\delta^{13}C$ would reflect mixing of organic and bottom-water carbon[31]. The excess CO_2 produced would also enhance $CaCO_3$ dissolution, which has been shown to cause lowering of Ba/Ca and Cd/Ca ratios[32], driving them towards Holocene-like values.

A reduction of the NADW flux and its associated ^{231}Pa load to the glacial Southern Ocean would increase the pool of ^{231}Pa remaining

in the glacial North Atlantic, suggesting an expected glacial pattern of higher North Atlantic and lower South Atlantic $^{231}Pa/^{230}Th$ ratios. Because $^{231}Pa/^{230}Th$ ratios in sediments co-vary with particle flux as well as with water column ^{231}Pa activity, this pattern might be reversed by changes in particle flux. Enhanced biological activity along glacial North Atlantic continental or ice margins would increase boundary scavenging of ^{231}Pa, leading to a depletion of ^{231}Pa at the middle ocean sampling sites of Yu *et al.*[9], which might buffer the $^{231}Pa/^{230}Th$ ratios to Holocene values (R.F. Anderson, personal communication). In the Southern Ocean, higher glacial diatom productivity near the sample sites (proximal to the Polar Front) would enhance delivery of ^{231}Pa to sediments and counter the effect of reduced import of ^{231}Pa via NADW. Some Southern Ocean studies have interpreted $^{231}Pa/^{230}Th$ ratio variations as reflecting productivity changes[33,34]. A recent study[34] concluded that $^{231}Pa/^{230}Th$ ratios in Southern Ocean sediments are insensitive to changes in NADW production.

Nd isotope ratios remain unfractionated by productivity changes, but reflect the ages of the continental sources. The simplest explanation for the Nd isotope variations is a decreased NADW flux during cold stages. This, coupled with increased glacial biological productivity, could reconcile the various proxy data for the Southern Ocean. □

Received 18 May 1999; accepted 25 April 2000.

1. Broecker, W. S. & Denton, G. H. The role of ocean-atmosphere reorganizations in glacial cycles. *Geochim. Cosmochim. Acta* **53**, 2465–2501 (1989).
2. Curry, W. B. & Lohmann, G. P. Reduced advection into Atlantic Ocean deep eastern basins during last glaciation maximum. *Nature* **308**, 317–342 (1983).
3. Oppo, D. W. & Fairbanks, R. G. Variability in the deep and intermediate water circulation of the Atlantic Ocean during the past 25,000 years: Northern Hemisphere modulation of the Southern Ocean. *Earth Planet. Sci. Lett.* **86**, 1–15 (1987).
4. Charles, C. D. & Fairbanks, R. G. Evidence from Southern Ocean sediments for the effect of North Atlantic deep-water flux on climate. *Nature* **355**, 416–419 (1992).
5. Labeyrie, L. *et al.* Hydrographic changes of the Southern Ocean (southeast Indian sector) over the last 230 kyr. *Paleoceanography* **11**, 57–76 (1996).
6. Charles, C. D., Lynch-Stieglitz, J., Ninnemann, U. S. & Fairbanks, R. G. Climate connections between the hemisphere revealed by deep sea sediment core/ice core correlations. *Earth Planet. Sci. Lett.* **142**, 19–27 (1996).
7. Lea, D. W. & Boyle, E. A. Foraminiferal reconstruction of barium distributions in water masses of the glacial ocean. *Paleoceanography* **5**, 719–742 (1990).
8. Boyle, E. A. Cadmium and $\delta^{13}C$ paleochemical ocean distributions during the Stage 2 glacial maximum. *Annu. Rev. Earth Planet. Sci.* **20**, 245–87 (1992).
9. Yu, E. -F., Francois, R. & Bacon, M. P. Similar rates of modern and last glacial ocean thermohaline circulation inferred from radiochemical data. *Nature* **379**, 689–694 (1996).
10. Albarède, F. & Goldstein, S. L. World map of Nd isotopes in sea-floor ferromanganese deposits. *Geology* **20**, 761–761 (1992).
11. Albarède, F., Goldstein, S. L. & Dautel, D. The neodymium isotopic composition of manganese nodules from the Southern and Indian oceans, the global oceanic neodymium budget, and their bearing on deep ocean circulation. *Geochim. Cosmochim. Acta* **61**, 1277–1291 (1997).
12. Piepgras, D. J. & Wasserburg, G. J. Isotopic composition of neodymium in waters from the Drake Passage. *Science* **217**, 207–214 (1982).
13. Jeandel, C. Concentration and isotopic composition of Nd in the South Atlantic Ocean. *Earth Planet. Sci. Lett.* **117**, 581–591 (1993).
14. Stordal, M. C. & Wasserburg, G. J. Neodymium isotopic study of Baffin Bay water: sources of REE from very old terranes. *Earth Planet. Sci. Lett.* **77**, 259–272 (1986).
15. Piepgras, D. J. & Wasserburg, G. J. Rare earth element transport in the western North Atlantic inferred from Nd isotopic observations. *Geochim. Cosmochim. Acta* **51**, 1257–1271 (1987).
16. Piepgras, D. J. & Jacobsen, S. B. The isotopic composition of neodymium in the North Pacific. *Geochim. Cosmochim. Acta* **52**, 1373–1381 (1988).
17. Levitus, S., Burgett, R. & Boyer, T. *World Ocean Atlas 1994: Nutrients* (US Department of Commerce, Washington DC, 1994).
18. Tucholke, B. E. & Embley, R. W. in *Interregional Unconformities and Hydrocarbon Accumulation* (ed. Schlee, J. S.) 145–164 (American Association of Petroleum Geologists, Tulsa, 1984).
19. Boyle, E. A. & Keigwin, L. North Atlantic thermohaline circulation during the past 20,000 years linked to high-latitude surface temperature. *Nature* **350**, 35–40 (1987).
20. Matsumoto, K. & Lynch-Stieglitz, J. Similar glacial and Holocene deep water circulation inferred from southeast Pacific benthic foraminiferal carbon isotope composition. *Paleoceanography* **14**, 149–163 (1999).
21. Pudsey, C. J. & Howe, J. A. Quaternary history of the Antarctic Circumpolar Current: evidence from the Scotia Sea. *Mar.Geol.* **148**, 83–112 (1998).
22. Petit, J. R. *et al.* Palaeoclimatological and chronological implications of the Vostok core dust record. *Nature* **343**, 56–58 (1990).
23. Basile, I. *et al.* Patagonian origin of glacial dust deposited in East Antarctica (Vostok and Dome C) during glacial stages 2, 4 and 6. *Earth Planet. Sci. Lett.* **146**, 573–589 (1997).
24. Jones, C. E., Halliday, A. N., Rea, D. K. & Owen, R. M. Neodymium isotopic variations in North Pacific modern silicate sediment and the insignificance of detrital REE contributions to seawater. *Earth Planet. Sci. Lett.* **127**, 55–66 (1994).
25. Jeandel, C., Bishop, J. K. & Zindler, A. Exchange of neodymium and its isotopes between seawater and small and large particles in the Sargasso Sea. *Geochim. Cosmochim. Acta* **59**, 535–547 (1995).
26. Fowler, S. W. *et al.* Rapid removal of Chernobyl fallout from Mediterranean surface waters by biological activity. *Nature* **329**, 56–58 (1987).
27. Abouchami, W., Goldstein, S. L., Galer, S. J. G., Eisenhauer, A. & Mangini, A. Secular changes of Pb and Nd isotopes in central Pacific seawater as recorded by a Mn crust. *Geochim. Cosmochim. Acta* **61**, 3957–3974 (1997).
28. Broecker, W. S. & Peng, T.-H. *Tracers in the Sea* (Eldigio, Palisades, New York, 1982).
29. Schmitz, W. *On the World Ocean Circulation: the Pacific and Indian Oceans* (Technical Report WHOI 96–08, Woods Hole Oceanographic Institution, 1996).
30. Lea, D. W. A trace metal perspective on the evolution of Antarctic Circumpolar Deep Water Chemistry. *Paleoceanography* **4**, 733–747 (1995).
31. Mackensen, A., Hubberten, H. -W., Bickert, T., Fischer, G. & Futterer, D. K. The $\delta^{13}C$ in benthic foraminiferal tests of Fontbiotia Wuellerstorfi (Schwager) relative to the $\delta^{13}C$ of dissolved inorganic carbon in Southern Ocean deep water: implications for glacial ocean circulation models. *Paleoceanography* **8**, 587–610 (1993).
32. McCorckle, D. C. Evidence of a dissolution effect on benthic foraminiferal shell chemistry: $\delta^{13}C$, Cd/Ca, Ba/Ca, and Sr/Ca results from the Ontong Java Plateau. *Paleoceanography* **10**, 699–714 (1995).
33. Kumar, N. *et al.* Increased biological productivity and export production in the glacial Southern Ocean. *Nature* **378**, 675–679 (1995).
34. Asmus, T. *et al.* Variations of biogenic particle flux in the southern Atlantic section of the Subantarctic Zone during the late Quaternary: evidence from $^{231}Pa_{ex}$ and $^{230}Th_{ex}$. *Mar. Geol.* **159**, 63–78 (1998).

Acknowledgements

We thank R. Anderson, W. Broecker, L. Burckle and N. Frank for discussions; J. Lynch-Stieglitz for providing the benthic $\delta^{13}C$ stratigraphy of RC11-83; and D. Hodell for sharing the stratigraphy of TNO57-6PC. R.R. thanks M. Fleisher, G. Hemming, M. Klas-Mendelson, and G. Mandal for help in the laboratory. We also thank A.N. Halliday for comments on the manuscript. This work was partly supported by the NSF and NOAA.

Correspondence and requests for materials should be addressed to S. L. G. (e-mail: steveg@ldeo.columbia.edu).

Mapping the Hawaiian plume conduit with converted seismic waves

X. Li*†, R. Kind*†, K. Priestley‡, S. V. Sobolev*, F. Tilmann‡, X. Yuan*† & M. Weber*§

** GeoForschungsZentrum Potsdam, Telegrafenberg, 14473 Potsdam, Germany*
† Freie Universität, FR Geophysik, Malteserstr. 74-100, 12249 Berlin, Germany
‡ Bullard Laboratories, Department of Earth Sciences, University of Cambridge, Cambridge CB3 0EZ, UK
§ Universität Potsdam, Institut für Geowissenschaften, Postfach 601553, 14415 Potsdam, Germany

The volcanic edifice of the Hawaiian islands and seamounts, as well as the surrounding area of shallow sea floor known as the Hawaiian swell, are believed to result from the passage of the oceanic lithosphere over a mantle hotspot[1–3]. Although geochemical and gravity observations indicate the existence of a mantle thermal plume beneath Hawaii[4–6], no direct seismic evidence for such a plume in the upper mantle has yet been found. Here we present an analysis of compressional-to-shear (P-to-S) converted seismic phases, recorded on seismograph stations on the Hawaiian islands, that indicate a zone of very low shear-wave velocity ($< 4\,km\,s^{-1}$) starting at 130–140 km depth beneath the central part of the island of Hawaii and extending deeper into the upper mantle. We also find that the upper-mantle transition zone (410–660 km depth) appears to be thinned by up to 40–50 km to the south-southwest of the island of Hawaii. We interpret these observations as localized effects of the Hawaiian plume conduit in the asthenosphere and mantle transition zone with excess temperature of ~300 °C. Large variations in the transition-zone thickness suggest a lower-mantle origin of the Hawaiian plume similar to the Iceland plume[7], but our results indicate a 100 °C higher temperature for the Hawaiian plume.

Evidence has recently been reported for seismic velocity anoma-